Teleoperated and Automatic Nanomanipulation Systems using Atomic Force Microscope Probes

Metin Sitti
Dept. of Mechanical Engineering and The Robotics Institute, Carnegie Mellon University
msitti@andrew.cmu.edu

Abstract

Nanomanipulation as a new emerging area enables to change, interact and control the nanoscale phenomenon precisely. In this paper, teleoperated and automatic control strategies for Atomic Force Microscope (AFM) probe based nanomanipulation applications are introduced. Teleoperated touching to silicon surfaces at the nanoscale is realized using a scaled bilateral force-reflecting servo type teleoperation control with custom-made 1 d.o.f. haptic device and AFM system. 1-D nanoforce sensing on the operator's finger is achieved during vertical or horizontal motion of the AFM probe tip on surfaces. Then, automatic constant height and force control strategies are introduced for pushing nanoparticles and indenting soft surfaces. 14nm radius gold nanoparticles are successfully positioned with few nanometers resolution, and wax surface is indented with a conical AFM tip. Finally, major nanoscale control challenges are reported.

Keywords: Nanorobotics, nanoscale systems and control, nanomanipulation, Atomic Force Microscopy.

1 Introduction

Nanotechnology which aims at the ideal miniaturization of devices and machines down to atomic and molecular sizes has been a recent hot topic as a promising key technologies in this century. However, for novel nanotechnology products, still there are many challenges to be solved in the nano world, and nanomanipulation is one of the key challenges [1]. Nanomanipulation is defined as the manipulation of *nanometer* size objects with a *nanometer* size end-effector with *(sub)nanometer* precision. By manipulation, it is meant that nanoobjects are pushed or pulled, cut, picked and placed, positioned, oriented, assembled, indented, bent, twisted, etc. by controlling external forces with sensory feedback. A basic nanomanipulation system structure is illustrated in Figure 1.

This paper is focused mainly on developing control strategies for nanomanipulation systems [2]. Main

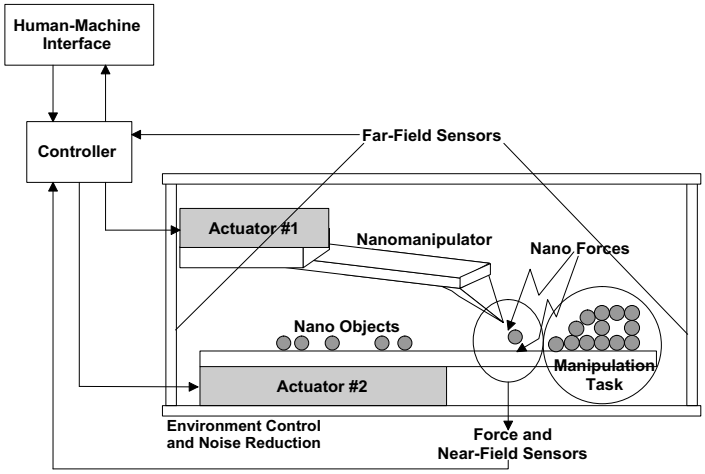

Figure 1: Basic structure of a generic nanomanipulation system.

manipulation tasks are limited to some mechanical tasks such as pushing/pulling, indenting, and touching. As the control approaches, teleoperated and semi-autonomous control strategies as shown in Figure 2 are investigated. In the former approach, a human operator directly in the control-loop manipulates the nanoobjects by using a man-machine user interface. Here, the operator controls the nanorobot directly or sends task commands to the nanorobot controller. Hollis et al. [3] used teleoperation control for tactile feedback from the nano world for the first time. In [4], [5], [6] and [7], force feedback and 3D real-time Virtual Reality graphics display interface are utilized during teleoperation. Direct teleoperation approach can realize tasks requiring high-level intelligence and flexibility. However, it is slow, not precise, not exactly repeatable, and engaged in many complex and challenging scale difference problems. On the other hand, the task-oriented approach avoids these problems by executing only the given tasks in a closed-loop autonomous control [8]. In the automatic control approach, nanorobot has a closed-loop control using sensory information without any user intervention. However, the automatic control in the nano world is still very challenging due to the complexity of the

nanoscale dynamics, no available real-time nanoscale visual feedback in ambient conditions, changing and uncertain physical parameters and disturbances, and insufficient models and intelligent strategies [9].

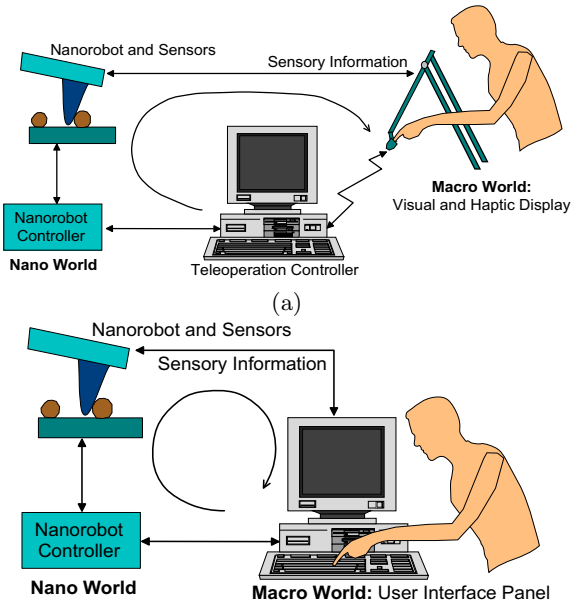

Figure 2: Nanomanipulation control approaches: (a) direct teleoperation control; (b) semi-autonomous (task-oriented) control.

2 Direct Teleoperation Control

Atomic Force Microscope (AFM) probe with its sharp tip is replaced by our finger at the nanoscale. For feeling the scaled nanoforces on the human finger, a bilateral teleoperation control system shown in Figure 3 is proposed. In this 1-D force-reflecting servo type system, the operator controls the slave AFM probe z position while feeling the resulting scaled perpendicular nanoscale forces in her/his finger using a bilateral controller. A 1 degree of freedom haptic device [4] is used as the master device. The operator pushes the bar of the haptic device, and the applied operator force f_m, measured by a strain gage full bridge sensor, moves the bar down to a position x_m which is measured by a position sensor. Then, the nanoprobe z position x_s is controlled using a proportional-integral (PI) controller so that it can track the scaled master device position $\alpha_p x_m$. The new x_s position results in a nanoforce of f_s on the surface, and scaled nanoforce $\alpha_f f_s$ and master force difference is used to calculate the linear motor torque using a proportional-derivative (PD) controller. This torque enables the force feedback in the operator finger.

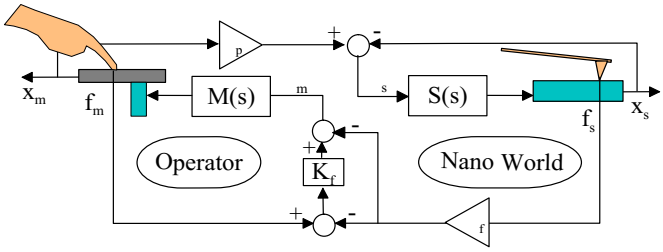

Figure 3: Scaled bilateral teleoperation control system.

The ideal response of the controller is given as follows [10]:

$$\begin{aligned} x_s &\rightarrow \alpha_p x_m \\ f_m &\rightarrow \alpha_f f_s \end{aligned} \tag{1}$$

at the steady state. Here $\alpha_f > 0$ and $\alpha_p > 0$ are the constant force and position scaling factors respectively. As the controller, a force-reflecting servo type controller is selected such that

$$\begin{aligned} \tau_m &= -\alpha_f f_s - K_f(\alpha_f f_s - f_m) \\ \tau_s &= K_v(\alpha_p \dot{x}_m - \dot{x}_s) + K_p(\alpha_p x_m - x_s) \end{aligned} \tag{2}$$

where K_p and K_v are proportional and differential control coefficients, and K_f is the force error gain. Using the slave and master dynamics equations, and assuming a very high tip-surface interaction stiffness such that $k_i >> k_c$, and $f_s = k_c x_s$, equalities for the ideal response at the steady state are given as follows:

$$\begin{aligned} \frac{x_s}{x_m} &= \alpha_p \frac{K_p}{1+K_p} \\ \frac{f_m}{f_s} &= \frac{1+K_p}{k_c \alpha_p K_f K_p} + \alpha_f\left(1+\frac{1}{K_f}\right) . \end{aligned} \tag{3}$$

Thus, for enabling the ideal responses, K_p and K_f should be selected as large as possible while they are upper bounded due to the stability conditions.

2.1 Experiments

During the experiments, a custom-made AFM system and 1 d.o.f. haptic device are utilized [8],[11]. The overall hardware setup of the experiments can be seen in Figure 4. Using this setup, two main types of experiments are realized: single-asperity (1-D) and surface (2-D) topography and compliance feedback.

2.1.1 Single-Asperity Contact Feedback

As an example of the teleoperated nanoscale touch experiment results, silicon AFM tip approached and retracted from a silicon (100) flat substrate. The AFM

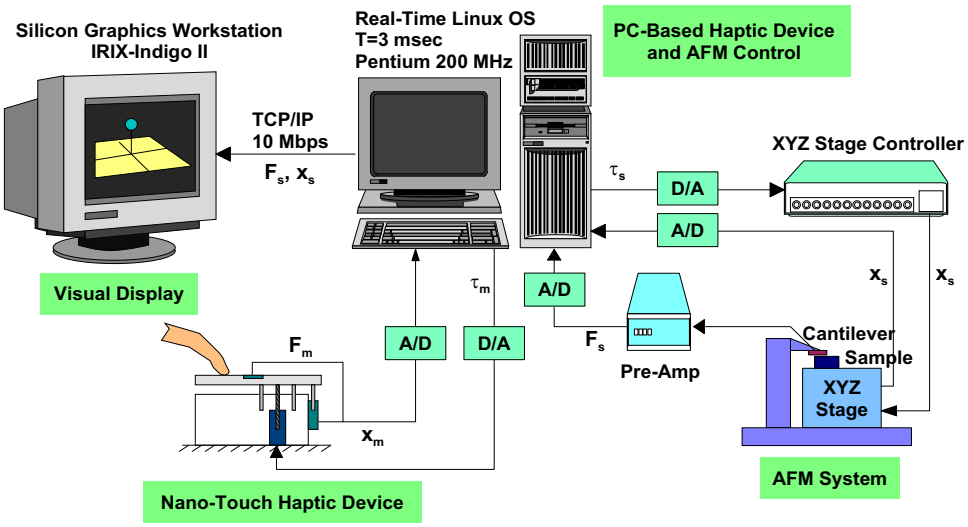

Figure 4: Experimental system setup for the teleoperated nanoscale touch feedback applications using the custom-made AFM and 1 d.o.f. haptic device.

probe has 20nm tip radius and 8N/m probe stiffness. Touching to the silicon sample at the 40% humidity conditions, resulting master and scaled slave position and forces can be seen in Figure 5. Experimental parameters are $K_f = 2$, initial tip height 0.6 μm, $\alpha_p = 4 \times 10^{-3}$ and $\alpha_f = 2.0 \times 10^6$. As can be seen from the figure, ideal responses of tracking the master and scaled slave forces and positions are realized successfully. The negative attractive forces are significantly large enough to feel the sticking to the surface. However, this sticking effect is small during the approach, and very large when retracting back. The reason is the adhesion force which results in an increased attractive force during separation. This difference causes of the force tracking error during the approach phases since the force occurs only very close to the surface (20-50nm). However, there is almost no tracking error for the positions since the piezoelectric z stage and the haptic device have the same bandwidth of 33Hz, and z stage is controlled in closed-loop.

2.1.2 Surface Tactile Feedback

In this experiment, surface forces and topographies are felt on the operator's hand while moving on the sample surface in $x-y$ coordinates. At first, the cantilever tip is approached to the surface, and put in contact with the substrate. Then, by controlling the $x-y$ AFM cantilever motion, the operator can feel the contact nanoforces and surface topography by the bilateral teleoperation controller during the $x-y$ motion. As the experimental result, silicon square gratings (TGZ-03 grating, Silicon-MDT Inc.), which are seen in the optical microscope top view image as in Figure 6a, is scanned along the line shown in the figure. The resulting tactile-sensing with the scale parameters of $\alpha_p = 10^{-6}$ and $\alpha_f = 1 \times 10^6$, and the force error gain of $K_f = 10$ is given in Figure 6b. The upward jumps stand for the silicon grid structures of 480 nm height. Here, the nanoobjects are assumed to be fixed on the substrate since the touching operation could move the non-fixed nanoobjects on the substrate by the applied pushing/pulling forces. However, if the objects are not completely fixed, the same operation could be utilized to manipulate them.

3 Semi-Autonomous Control

In this part, as automatic manipulation tasks, nanoparticles semi-fixed to a flat substrate are to be pushed precisely and soft surfaces are to be indented using an AFM probe tip in ambient conditions. At first, 3-D images of surfaces are obtained using the AFM tapping-mode imaging technique [11]. Then, the particles to be pushed, or the surface points to be indented are determined by a user, and the AFM probe controller realizes the task automatically.

3.1 Precise Positioning of Nanoparticles

AFM probe based positioning of nanoparticles is realized by the contact pushing of the particles. Automatic 1-D pushing strategy is given in Figure 7 as:

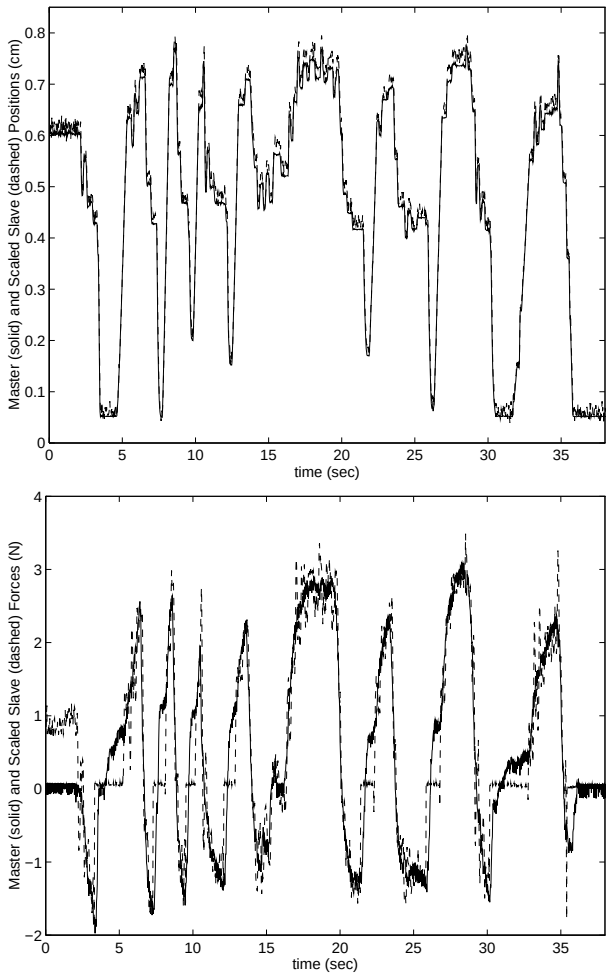

Figure 5: Single-asperity touching experimental results to a silicon surface with an AFM probe tip: master (solid) and scaled slave (dashed) position (upper) and forces (lower). In the force plot, negative forces correspond to the attractive approach or separation forces while positive ones do the repulsive contact forces.

- $1 \rightarrow 2$ (*auto-parking*): the AFM tip is automatically moved at the z-direction until detecting the contact by the substrate by measuring the cantilever deflection, and retracted back to a predetermined parking height h_{set}.
- $2 \rightarrow 3$ (*automatic tip-particle contact detection*): the tip is moved along the substrate until detecting the particle by cantilever deflection detection, and then stopped.
- $3 \rightarrow 4$: pushing the particle for a desired distance Δy by moving the substrate (or the tip) with a constant speed,
- $4 \rightarrow 5$: after completing the pushing operation, retracting back to the initial height.

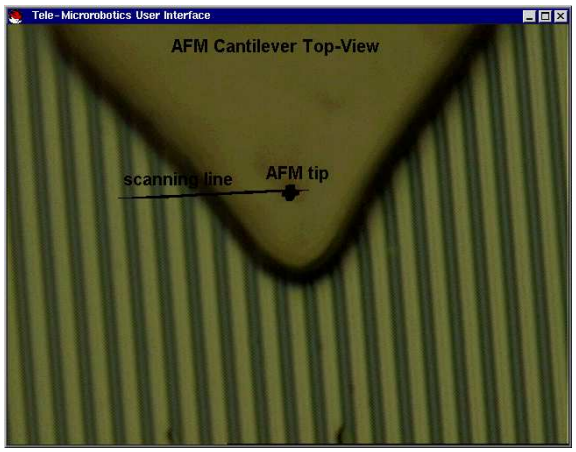

(a)

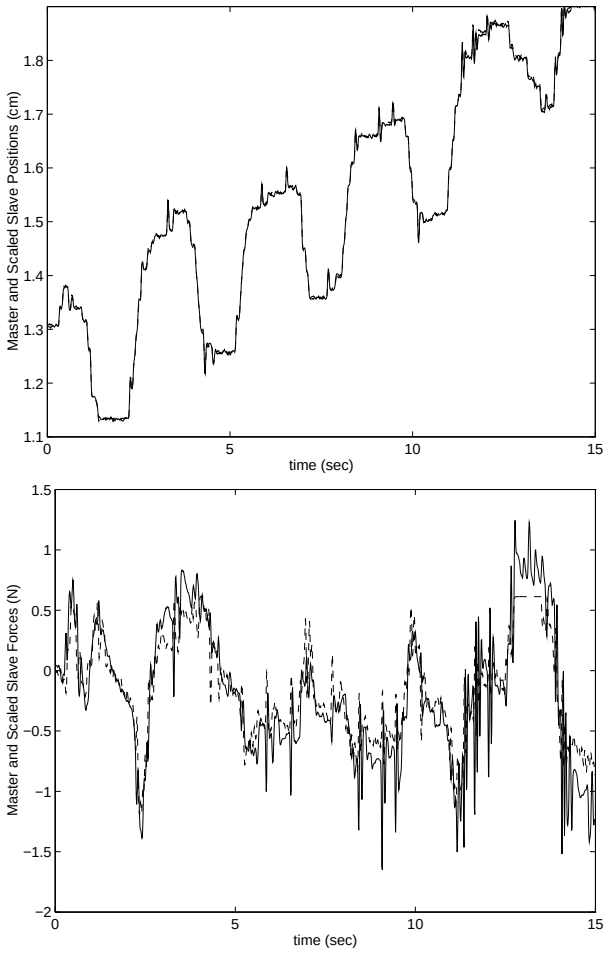

(b)

Figure 6: (a) Silicon grids with 480 nm height and 3 μm pitch are felt along the black line, and (b) resulting topology and force feedback using the force reflecting servo type controller: scaled slave (dashed line) and master (solid line) positions (upper) and forces (lower).

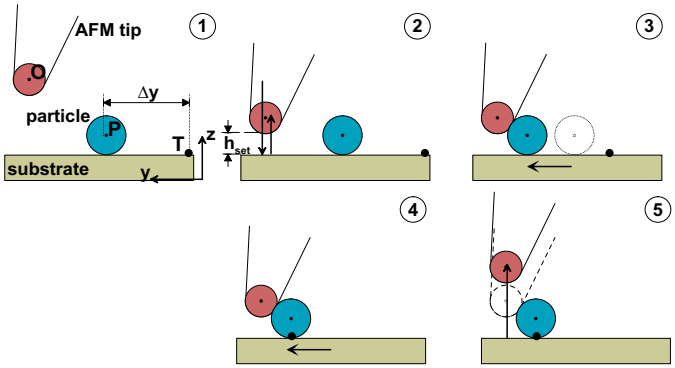

Figure 7: AFM-based automatic 1D particle pushing strategy: 1 → 2: automatic parking, 2 → 3: tip-particle contact detection, 3 → 4: pushing, and 4 → 5: tip retraction.

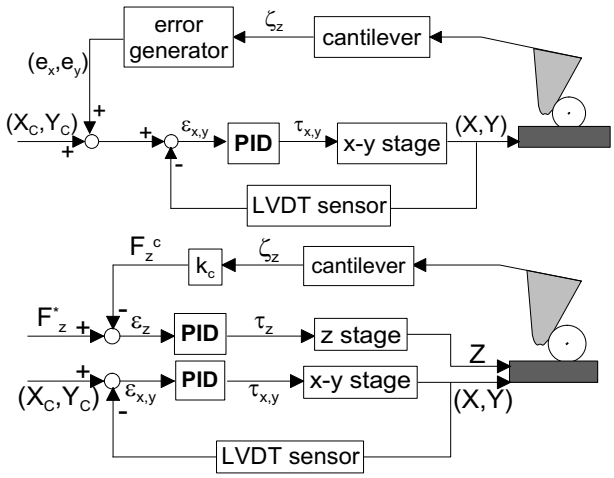

Figure 8: Automatic pushing control schemes for precise nanoparticle positioning: constant height control (upper) and constant contact force control (lower) strategies.

Since there is no real-time visual feedback of the particle position in ambient conditions, only the real-time force feedback from the AFM probe deflection could be utilized during the pushing operation. As pushing control strategies, two different automatic control strategies illustrated in Figure 8 are considered: *constant height* and *constant contact force* controls. The former strategy controls the stage z position to keep at the reference height using a LVDT (linear variable differential transformer) position sensor integrated to the stage z-axis, and measures the probe deflection, e.g. force, during pushing. This technique assumes the substrate is very flat. It is especially useful for characterizing the frictional behavior between the nanoparticle and substrate interfaces [12] by measuring the forces during pushing. However, it cannot compensate errors due to the substrate random height or orientation differences. In the latter approach, the pushing operation is not affected by the substrate surface topography changes, or the substrate surface alignment errors. However, the only problem arises if the tip slips from the particle surface, and contacts with the substrate instead of the particle during pushing. This case could be rare for a sliding type of particle motion, but it becomes possible if the particle rolls. Slow pushing, and careful design of the tip-particle friction/sticking can eliminate this problem.

As experimental results using the constant height control technique, 14nm radius gold particles semi-fixed on a mica substrate [13] are positioned precisely as shown in Figure 9. By this technique, few nanometers precision positioning of nanoparticles is possible.

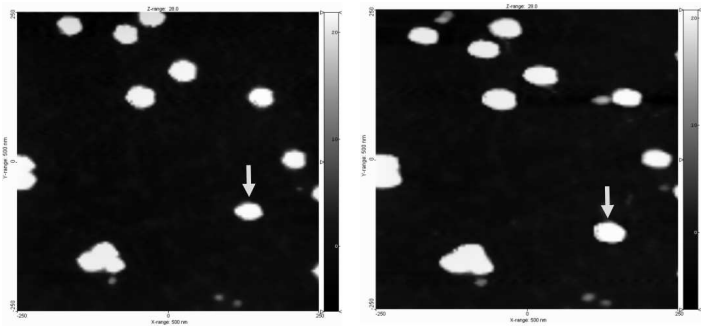

Figure 9: Constant height control based autonomous pushing of a 14nm radius gold nanoparticle with an AFM probe: before (left) and after (right) pushing (500nm × 500nm × 28nm scan size).

3.2 Nanoindentation of Surfaces

In order to fabricate nanostructures similar to the AFM probe tip shape, a soft surface such as a polymer [14] or wax [15], [16] is indented vertically with a given tip shape, e.g. conical, pyramidal, cylindrical, etc. Operator chooses an x-y point to indent, and an automatic controller controls the z position of the probe (or sample) to indent the surface with a reference indentation depth. Since the initial tip height is not known, contact point is determined and the tip is positioned to a predetermined height. Then, the force feedback from the AFM probe deflection is used to detect the starting of the indentation, and stopping it after reaching to the target depth.

4 Conclusions

Teleoperated and autonomous control techniques for AFM probe based surface topography and elastic-

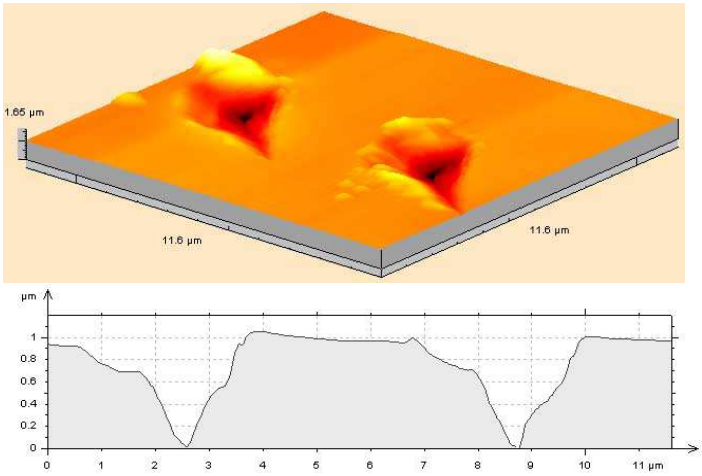

Figure 10: Autonomous indentation of a wax surface using an AFM probe: AFM images of the indented surface (upper) ($11.6\mu m \times 11.6\mu m \times 1.65\mu m$ scan size), and the profile of the indented probe tip shape (lower) [15].

ity feedback, nanoparticle pushing, and surface indenting are proposed in this paper. Each control technique is utilized for experimental validation of the success of the proposed controllers. 1-D and 2-D force feedback from silicon flat and grid surfaces are achieved, 14nm radius gold nanoparticles on mica substrates are pushed with few nanometers precision, and wax surfaces are indented with a controlled depth successfully. Main challenges of nanoscale manipulation control using AFM probes can be summarized as follows:

- Real-time visual feedback at the nanoscale systems in ambient conditions is very challenging, and mostly other sensory information should be used to control the AFM probe. Real-time force feedback is the most advantageous for AFM probes while the force feedback information includes limited knowledge about the AFM probe tip position and forces on the nanoobject and substrate. Therefore, modeling of AFM probe tip and nanoobject interaction is required for measuring various position and force parameters indirectly.
- Actuator nonlinearity, parameter uncertainties, and extreme sensitivity to disturbances are challenging issues to be solved for stable and robust control.
- For teleoperated nano-manipulation, force scaling laws for reliable nanoscale force feedback are to be defined analytically for a stable and transparent force-reflecting interaction.

References

[1] D. M. Eigler and E. K. Schweitzer, "Positioning single atoms with a scanning electron microscope," *Nature*, pp. 524–526, Apr. 1990.

[2] M. Sitti, "Survey of nanomanipulation systems," *IEEE Nanotechnology Conference*, pp. 75–80, Maui, USA, 2001.

[3] R. L. Hollis, S. Salcudean, and D. W. Abraham, "Toward a tele-nanorobotic manipulation system with atomic scale force feedback and motion resolution," in *Proc. of the IEEE Int. Conf. on MEMS*, pp. 115–119, 1990.

[4] M. Sitti and H. Hashimoto, "Tele-nanorobotics using atomic force microscope as a robot and sensor," *Advanced Robotics Journal*, vol. 13, no. 4, pp. 417–436, 1999.

[5] M. Falvo, R. Superfine, S. Washburn, and et al., "The nanomanipulator: A teleoperator for manipulating materials at the nanometer scale," in *Proc. of the Int. Symp. on the Science and Technology of Atomically Engineered Materials*, pp. 579–586, Richmond, USA, Nov 1995.

[6] M. Sitti and H. Hashimoto, "Teleoperated touch feedback from surfaces at the nanoscale: Modeling and experiments," in *IEEE/ASME Tran. on Mechatronics*, March 2003 (to appear).

[7] M. Sitti, B. Aruk, K. Shintani, and H. Hashimoto, "Scaled Teleoperation System for Nanoscale Interaction and Manipulation," in *Advanced Robotics Journal*, March 2003 (to appear).

[8] M. Sitti and H. Hashimoto, "Two-dimensional fine particle positioning under optical microscope using a piezoresistive cantilever as a manipulator," *Journal of Micromechatronics*, vol. 1, no. 1, pp. 25–48, 2000.

[9] M. Sitti and H. Hashimoto, "Teleoperated nanoscale object manipulation," in *Recent Advances on Mechatronics*, pp. 322–335, ed. by O. Kaynak, S. Tosunoglu and M.J. Ang, Springer Verlag Pub., Singapore, 1999.

[10] Y. Yokokohji and T. Yoshikawa, "Bilateral control of master-slave manipulators for ideal kinesthetic coupling–formulation and experiment," *IEEE Trans. on Robotics and Automation*, vol. 10, pp. 605–619, Oct. 1994.

[11] M. Sitti and H. Hashimoto, "Controlled pushing of nanoparticles: Modeling and experiments," *IEEE/ASME Trans. on Mechatronics*, vol. 5, pp. 199–211, June 2000.

[12] M. Sitti, "Nanotribological Characterization System by AFM Probe based Controlled Pushing," in *IEEE/ASME Tran. on Mechatronics*, Sept. 2002 (under review).

[13] R. Resch, C. Baur, and et al., "Manipulation of nano particles using dynamic force microscopy: Simulation and experiments," *Appl. Phys. A*, vol. 67, pp. 265–271, Sept. 1998.

[14] U. Drechsler, U. Durig, B. Gotsmann, W. Haberle, M.A. Lantz, H.E. Rothuizen, R. Stutz, and G.K. Binnig, "The Millipede-Nanotechnology entering data storage," *IEEE Trans. on Nanotechnology*, vol. 1, no. 1, pp. 39–55, March (2002).

[15] K. Autumn, M. Sitti, Y.A. Liang, A.M. Peattie, W.R. Hansen, S. Sponberg, T. Kenny, R. Fearing, J.N. Israelachvili, and R.J. Full, "Evidence for van der Waals attachment by gecko foot-hairs," *Proc. National Acad. Sciences*, **99**, 12252–12256 (2002).

[16] M. Sitti and R.S. Fearing, "Synthetic gecko foot-hair micro/nanostructures as dry adhesives," *Journal of Adhesion Science and Technology*, April 2003 (to appear).